ChemBioChem

Research Article
doi.org/10.1002/cbic.202400475

Chemistry Europe
European Chemical Societies Publishing

www.chembiochem.org

Complex Formation and Hydrolytic Processes of Protected Peptides Containing the –SXH– Motif in the Presence of Nickel(II) Ion

Balázs Sándor,[a] Ágnes Grenács,[a] Lajos Nagy,[b] Oldamur Hollóczki,[c] and Katalin Várnagy*[a]

Interactions between metal ions and proteins are considered reversible, such as the coordination of a metal ion to a protein or enzyme, but irreversible processes like the oxidative reactions, aggregation or hydrolytic processes may occur. In the presence of Ni(II)-ions selective hydrolysis of the peptides containing the –SXH– or –TXH– motif was observed. Since the side chain of histidine serves as the metal ion binding site for many native proteins, and very often histidine is present in a –SXH– or –TXH– sequence, to study the complex formation and hydrolytic processes in presence of nickel(II) ion four peptides were synthesised: Ac-SKHM-NH_2, A_3SSH-NH_2, A_4SSH-NH_2, AAAεKSH-NH_2. The Ni(II)-induced hydrolysis of Ac-SKHM-NH_2 peptide occurs rapidly in alkaline medium already at room temperature. In two peptides containing –SSH– sequence on the C-termini, the N-terminal part is the major binding site for the nickel(II) ion, but the formation of dinuclear complexes was also observed. In the $[Ni_2LH_{-6}]^{2-}$ complex of hexapeptide, the coordination sphere of the metal ions is saturated with deprotonated Ser-O^-, which does not result in hydrolysis of the peptide. For A_4SSH-NH_2, both Ni(II) ions fulfill the conditions for hydrolysis, which was confirmed by HPLC analyses at pH ≈8.2 and 25 °C.

Introduction

Transition metal ion–peptide interactions have been studied for more than 50 years. Research has been boosted by the development of automatic peptide synthesizer devices, including the production of shorter and longer fragments of various proteins, and by the results of research into neurodegenerative diseases, which have highlighted the possible role of both essential (Cu(II), Zn(II)) and toxic metal ions.

On the other hand, metal ion-peptide interactions very often involve not only complex formation but also metal ion-induced hydrolysis and metal ion-catalysed oxidation. Metal ion-induced hydrolysis has been studied for several metal ions, most extensively for Pd(II) and Pt(II) complexes. In general, it has been shown that Pd(II) and Pt(II) complexes are capable of hydrolytic cleavage of methionine- or histidine-containing peptides. The complexes bind to the heteroatom in the side chain of methionine or histidine and promote hydrolysis of the amide bond. In addition, the study of numerous dinuclear Pt(II) complexes has shown that these complexes are very effective in promoting the hydrolysis of amide bonds of methionine-containing peptides.[1–5]

Much less studies have been published with copper(II) ions, because it is significantly less involved in hydrolytic processes which are very slow. Cu(II) was found to induce the hydrolysis of peptides containing –SH– and –TH– sequences at a much higher rate than other histidine-containing peptides in slightly alkaline media. As with nickel(II), the reaction takes place exclusively in 4 N complexes. The maximum rate of the Cu(II)-dependent reaction is on average ca. 100 times lower than that of the Ni(II)-dependent one. Studies have shown that the specificity of SerHis and ThrHis sequences is 10–50 times greater than that of other histidine-containing peptides and more than 100 times greater than that of peptides without histidine.[6] On the other hand the greater ability of Cu(II) ions to form 4 N complexes at lower pH results in hydrolytic activity already around physiological pH (oH ≈ 7).[7]

Zn(II)-induced hydrolysis was detected for X-Ser dipeptides with a serine residue at the C-termini. In the presence of $ZnCl_2$ at pH 7, rapid hydrolysis of X-Ser occurs due to an autocatalysis of the hydroxyl group in the serine residue and was also found to be accelerated by the Zn(II) ions.[8]

Ni(II)-induced selective hydrolysis of peptide bonds has been studied in detail for oligopeptides with different, systematically designed amino acid sequences and subsequently for natural protein fragments. These studies have shown that Ni(II)-dependent hydrolysis of the peptide bond occurs in the amino acid sequences –Z^1**S**X**H**Z^2– or –Z^1**T**X**H**Z^2– (where Z^1 and Z^2 represent any amino acid residue and X represents any amino acid residue except proline). The hydrolysed bond is located

[a] B. Sándor, Á. Grenács, K. Várnagy
Inorganic and Analytical Chemistry, University of Debrecen, H-4032 Debrecen, Egyetem tér 1, Hungary
E-mail: varnagy.katalin@science.unideb.hu

[b] L. Nagy
Department of Applied Chemistry, University of Debrecen, H-4032 Debrecen, Egyetem tér 1. Hungary

[c] O. Hollóczki
Department of Physical Chemistry, University of Debrecen, H-4032 Debrecen, Egyetem tér 1. Hungary

Supporting information for this article is available on the WWW under https://doi.org/10.1002/cbic.202400475

between the Z^1 and serine/threonine. Ni(II) binding occurs by a planar 4 N coordination through a histidine imidazole-N and 3 preceding peptide N atoms.

This process causes a bending of the peptide chain and the nucleophilic Ser/Thr hydroxyl group becomes spactically close to the preceding peptide bond, resulting in the formation of an intermediate ester product, which undergoes spontaneous hydrolysis in aqueous solution (Scheme 1). Initially the previous studies of hydrolysis were performed generally at 45–50 °C, pH range 8.2–8.5.[9–13] However, in some cases the study was extended to lower temperatures and remarkably fast hydrolytic processes were observed.[14]

The –SXH– or –TXH– sequence, which is susceptible to Ni(II)-dependent hydrolysis, is present in many proteins (histone, annexin, zinc-finger protein, etc.) but only some of them can undergo Ni(II)-induced hydrolysis under physiological conditions. It has been shown that the type of amino acid residue near the potential hydrolysis site has a significant impact on the reaction rate. Bulky and hydrophobic side chains adjacent to the histidine residue promote a fast reaction.[15–17] The formation of an initial 4 N Ni(II) complex is a prerequisite for hydrolysis to occur, so the availability of the potential cleavage site to Ni(II) ions is necessary, and the pH required for complex formation is also crucial. The protein sequences harbouring cleavage sites must therefore be exposed at the protein surface and sufficiently flexible to adopt the square-planar structure of the complex, but a local bend in the protein backbone may predispose it into such a conformation, which enables a faster hydrolysis than that expected from the neat sequence alone.[18–21]

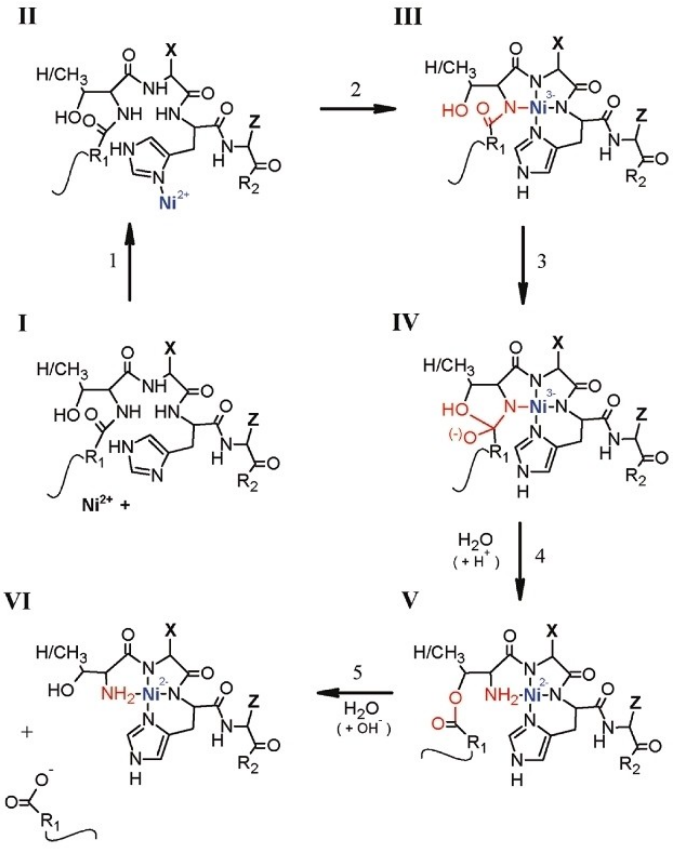

Scheme 1. Mechanism of Ni(II)-ion-induced hydrolysis of peptides containing-S/TXH-sequence.[10]

Over the past decades, our research group has carried out extensive research on interaction between transition metal ions and proteins associated with neurodegenerative diseases. We have studied first of all the complex formation processes of their peptide fragments containing metal ion binding sites with copper(II), nickel(II) and zinc(II) ions. Usually the side chain of histidine serves as the metal ion binding site for these proteins, and very often histidine is present in a specific amino acid environment, such as –SXH– or –TXH– sequence. Since peptides containing such sequences are involved not only in complex formation but also in hydrolytic processes in case of some metal ions, four peptides were synthesized to study complex formation and hydrolytic processes in the presence of nickel(II). Our aims were to determine whether Ni(II)-induced hydrolysis also occurs under conditions of potentiometric measurements (25 °C) and during their duration, which may affect the values of the stability constants determined from equilibrium measurements.

The investigated peptides include a simple tetrapeptide with the sequence Ac-SKHM-NH_2, representing the shortest ligand where only an acetyl group preludes the serine moiety. The further molecule (AAAASSH-NH_2, A_4SSH-NH_2) contains an N-terminal binding site as well, due to the free amino group behaving as an anchor for nickel(II) ions. Through these two peptides the preference of metal binding and its impact on hydrolytic reactions can also be studied. Moreover, a hexapeptide (AAASSH-NH_2, A_3SSH-NH_2) was also studied, in which there are fewer amide nitrogen donors of the peptide backbone, and the two metal binding regions cannot fill the coordination sphere of two nickel(II) ions. Since the mechanism of the hydrolysis of the peptide involves an intermediate ester species, an analogous ligand (AAAεKSH-NH_2, A_3εKSH-NH_2) with an identical structure apart from the replacement of the ester group to an alkyl chain of lysine was involved in the experiments. The structural formulae of peptides are shown in Figure 1.

Results and Discussion

Acid-Base Properties and Complex Formation Processes of Peptides

The processes occurring in solution in the presence of nickel(II) were investigated for four peptides: Ac-SKHM-NH_2, A_4SSH-NH_2, A_3SSH-NH_2 containing –SXH– motif and AAAεKSH-NH_2 representing the analogue molecule of the intermediate ester of the mechanism of peptide hydrolysis (see Figure 1). All peptides were examined by pH-potentiometry and the protonation and deprotonation constants (logβ and pK) of the ligands and the stability constants (logβ) values of their nickel(II) complexes are collected in Table 1 and 2.

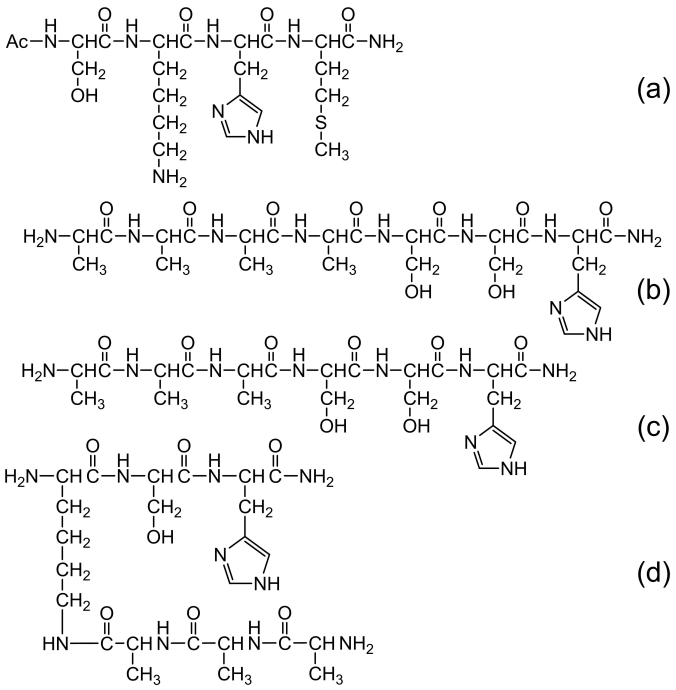

Figure 1. Structural formulae of the peptides: Ac-SKHM-NH_2 (a), A_4SSH-NH_2 (b), A_3SSH-NH_2 (c), A_3εKSH-NH_2 (d).

Protonation constants of the peptides corroborates literature data; each peptide contains a histidine residue, which has a protonation constant around 6.5.

Peptides with free amino terminus have a p*K* value around 8, which is identical to that of similar peptides, for example the tetrapeptide GTHS-NH_2, related to the ammonium function. The ε-Lys modified ligand has two amino groups resulting in an additional p*K* around 8. Ac-SKHM-NH_2 also contains an ε-amino group of a lysine moiety, having a p*K* around 11. (See structures in Figure 1.)

Mononuclear complexes are formed with all the mentioned peptides with similar stoichiometries. The hexa- and heptapeptides contain two metal binding sites; the amino terminus and the C-terminal imidazole side chain. Modelling their nickel binding environments, other peptides are listed in Table 2; formerly investigated GTHS-NH_2 and MKHM-NH_2 peptide representing the albumin (ATCUN motif) like coordinating site (NH_2,N^-,N^-,N_{Im}), AAAA tetraalanine-like coordinating site, while the hereby investigated Ac-SKHM-NH_2 contains a serine residue in the -SXH- motif, similarly to A_4SSH-NH_2 and A_3SSH-NH_2.

It also can be seen that only A_4SSH, A_3SSH and A_3εKSH ligands are able to bind two nickel(II) ions forming dinuclear species. In the absence of serine residues, precipitation occurred in the metal excess system of G_5H which can be due to the hydrolysis of unbound nickel(II) ions.[23]

Deacetylation Induced by Nickel(II)

For Ac-SKHM-NH_2 tetrapeptide, formerly investigated in the presence of copper(II), structural change was observed in complex geometry based on its CD spectra compared to other -XaaYaaHis- complexes (Xaa,Yaa≠His,Cys,Asp,Gly,Ser,Thr).[20] Nickel(II) complexes of the ligand show the expected stability values gained from pH potentiometric data; $[NiHL]^{3+}$, $[NiH_{-2}L]$ and $[NiH_{-3}L]^-$ species are present in solution representing cooperative deprotonation steps. It should be considered that a quite high p*K* value corresponds to the ε-ammonium group of lysine, meaning the formation of $[NiL(H)]^{3+}$, $[NiH_{-3}L(H)]$ and $[NiH_{-3}L]^-$, respectively, due to the protonated side chain in the former two complexes. Similarly to the one-histidine containing ligands studied earlier, $[NiL]^{2+}$ can be considered as having a monodentate bound metal ion to the imidazole nitrogen atom of histidine, and the subsequent deprotonation processes are related to the preceding amide nitrogen atoms forming a stable fused chelate system. The highest p*K* value represents the deprotonation of the lysine residue without further change in the coordination sphere of nickel(II). However, CD spectroscopic investigation of the complex formation processes of Ac-SKHM-NH_2 shows difference when compared to a non-serine analogue, Ac-MKHM-NH_2 (Figure 2).[23]

The appearance of a positive and a negative CD band can be observed which is a mirror image of the expected curve, when the -S/TXH- motif is not present. Interestingly, this anomaly results in an apparently similar CD spectrum to that of an albumin-like (NH_2,2 N^-,N_{im}) coordinated nickel(II) ion (Figure 2).[23] In order to ensure the non-reversible feature of the reaction, pH-dependent series of the spectra have been recorded again after re-acidification. CD activity appears at unambiguously lower pH showing similar CD bands as during

Table 1. Formation (logβ) and deprotonation constants (p*K*) of the studied ligands and some other peptides for comparison (T = 25 °C, I = 0.2 M KCl).

	Ac-SKHM-NH_2[22]	A_4SSH-NH_2	A_3SSH-NH_2	A_3εKSH-NH_2	GTHS-NH_2[23]	MKHM-NH_2[23]	AAAA[24]	G_5H[25]
[HL]	10.33	7.90(1)	8.00(1)	8.11(1)	7.95	10.18	8.13	8.00
[H_2L]	16.56(1)	14.25(1)	14.44(2)	15.51(1)	14.22	17.39	11.65	14.87
[H_3L]	–	–	–	21.78(1)	–	23.40	–	17.73
pK_{COOH}	–	–	–	–	–	–	3.52	2.86
pK_{Im}	6.23	6.35	6.44	6.27	6.27	6.01	–	6.87
pK_{NH2}	–	7.90	8.00	7.40	7.95	7.21	8.13	8.00
pK_{NH2}	–	–	–	8.11	–	–	–	–
pK_{Lys}	10.33	–	–	–	–	10.18	–	–

Table 2. Stability constants (logβ) and various derived constants of the nickel(II) complexes of studied ligands and some other peptides for comparison, T = 25 °C, I = 0.2 M.

	Ac-SKHM-NH_2	A_4SSH-NH_2	A_3SSH-NH_2	A_3εKSH-NH_2	GTHS-NH_2[23]	MKHM-NH_2[23]	AAAA[24]	G_5H[25]
[NiHL]	12.51(13)	–	–	–	–	13.20	–	–
[NiL]	5.04(7)	3.92(3)	4.69(3)	–	4.67	–	3.06	5.46
[NiL_2]	–	7.42(9)	8.68(10)	–	–	–	–	9.06
[$NiH_{-1}L$]	–	–	–	2.35(2)	–	2.62	−4.97	–
[$NiH_{-2}L$]	−10.78(3)	–	–	−5.21(10)	−6.45	−7.51	–	−10.75
[$NiH_{-3}L$]	−21.19(7)[a]	−20.38(3)	−19.76(4)	−15.45(12)	−17.6	–	−21.29	−19.94
[$Ni_2H_{-4}L$]	–	−25.81(6)[a]	−24.75(7)	–	–	–	–	
[$Ni_2H_{-5}L$]	–	–	–	−25.48(5)	–	–	–	–
[$Ni_2H_{-6}L$]	–	−41.69(2)[a]	−41.66(5)	–	–	–	–	–
lg*K*(Ni + L)	2.28	3.92	4.69	–	4.67	3.02	3.06	5.46
pK_{amid1}	7.47	8.10	8.15	(≈5.70)[b]	5.56	5.29	8.03	
pK_{amid2}	7.91						8.16	8.11
pK_{amid3}					–	–		9.19
pK_3	–	–	–	10.26	11.15	–	–	–
pK_{Lys}	10.41	–	–	–	–	10.13	–	–

[a] Species which can undergo hydrolysis causing uncertainty in the determined stability values
[b] The first pK value of the Ni(II):A_3εKSH-NH_2 system is an estimated value from the distribution curves.

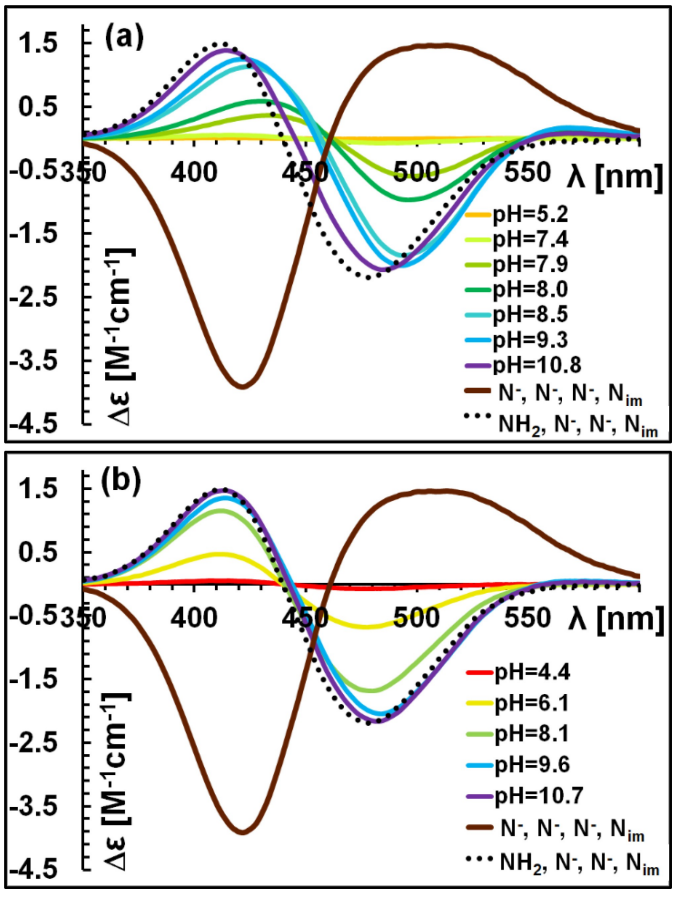

Figure 2. pH dependent CD spectra of the equimolar nickel(II) – Ac-SKHM-NH_2 system (a) and the repeated series of spectra after re-acidification (b) and that of the (3 N^-,N_{im}) coordinated Ni(II)-Ac-MKHM-NH_2 (data from ref. [23]) and (NH_2,2 N^-,N_{im}) coordinated Ni(II)-MKHM-NH_2 complex (data from ref. [23]).

the first CD titration, meaning that a more stable complexing ligand is present. This observation strengthens the former evidence of the formation of a different, albumin-like coordinating molecule, having a well-known and very high stability complex with nickel(II).

The unexpected series of CD curves was observed earlier for peptide fragments of some native proteins as well[20,26] and the nickel(II) induced specific cleavage of the investigated peptides was described.[8–19,24] The schematic reaction pathway can be seen in Figure S1, meaning the formation of an N-terminally free peptide and acetate ion as final products.

However, previously, hydrolytic processes have been studied at 37–45 °C and in the presence of twofold nickel(II) excess, whereas in the present case the peptide to nickel(II) ion molar ratio corresponds to the number of metal binding sites. Moreover, in previous cases an oligopeptide was cleaved from the –S/TXH- motif, while here only an acetate ion is the leaving group. Although, the change of donor atoms in the coordination sphere of nickel(II) complexes can be followed by its CD spectra, the totality of the reaction cannot be proved by only this technique, because the same environment is present in the intermediate ester and the final product. (Figure 2).

To prove the occurrence of the specific hydrolysis of the ligand, HPLC chromatograms were registered for the free ligand and after the titration of the equimolar nickel(II)–Ac-SKHM-NH_2 system (Figure 3). The initial peak of the ligand is almost vanished, while another peak appears at lower retention time. The formed reaction product is more polar than the Ac-SKHM-NH_2 ligand itself, correlating well with the different shape of CD spectra and the formerly supposed hydrolytic cleavage, since the deacetylation occurred forming a free amino group and an albumin-like coordination environment.

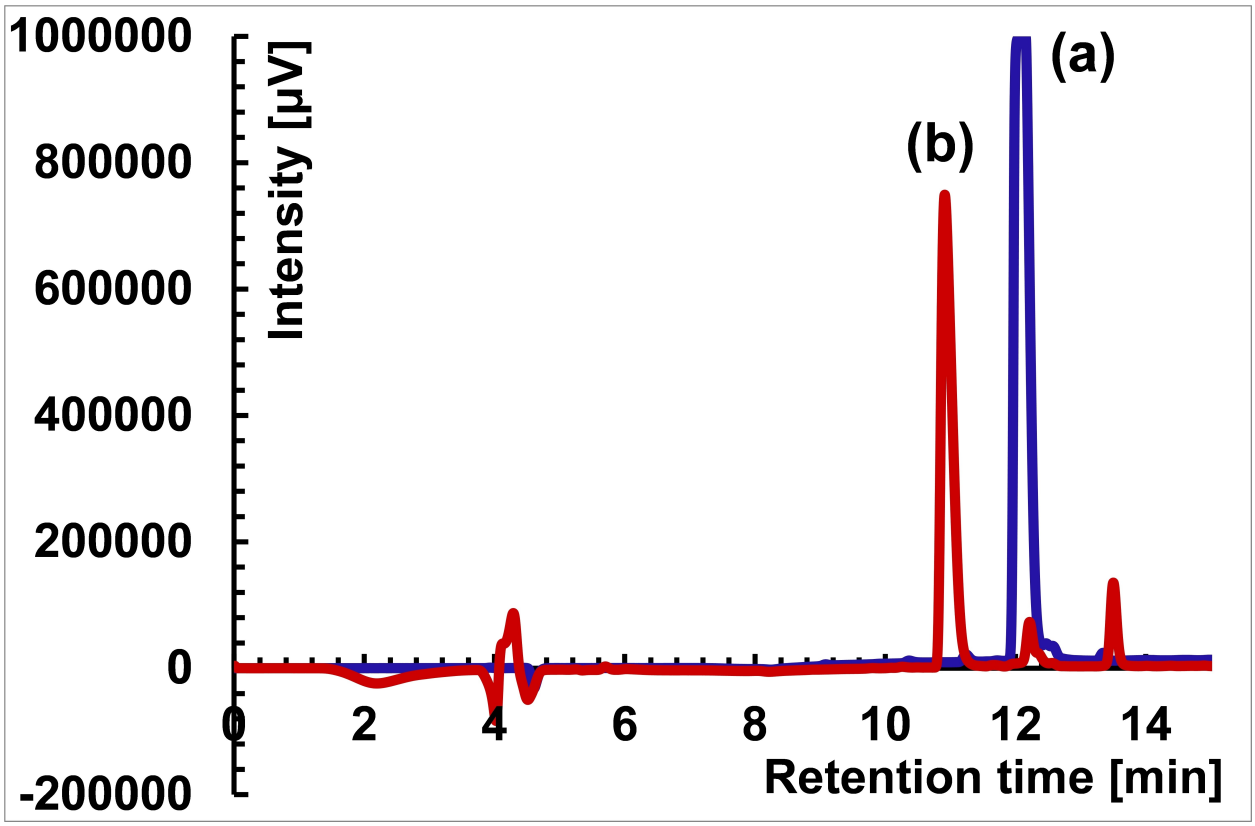

Figure 3. HPLC chromatogram of the free ligand (a) and the Ni(II):Ac-SKHM-NH_2 = 1 : 1 system after pH-potentiometric titration (b).

The time dependence was also investigated by CD spectroscopy in basic medium (pH = 9.69), where the nickel(II):ligand = 1 : 1 sample was analysed after titration and the CD curves were recorded at different elapsed times (Figure S2).

The figure clearly shows that the high intensity negative and positive Cotton effect (CE) gradually shifts to the lower wavelengths. After 50 min there is no further change in the spectra, so the coordination environment of nickel(II) at high pH does not change after one hour. This curve is in complete agreement with the CD spectrum of Ni(II) complexes with albumin-like (NH_2,N^-,N^-,N_{im}) coordination mode, which means that all the peptide is fully transformed to the mentioned coordination mode in one hour at 25 °C and pH = 9.69.

Altogether, these findings show that the interaction of nickel(II) and the short peptide is not only coordinative, but also non-reversible, caused by the cleavage of the peptide bond preceding the serine residue which can take place under the conditions of pH potentiometric titration, but only in high pH range. This also implies that the evaluation of titration data measured in the pH range below 8.5, the stability constants calculated for $[NiHL]^{3+}$, $[NiL]^{2+}$ and $[NiH_{-2}L]$ complexes formed in that range are correct thermodynamic data. This is also demonstrated by the fact that the stoichiometry and the stability of the formed species according to the data of titration does not show any difference compared to peptides having no -S/TXH- motif. The $[NiH_{-2}L]$ complex is the main species with (N^-,N^-,N^-,N_{im}) coordination mode. The next deprotonation step above pH 10 corresponds to the deprotonation of the ammonium group of the lysine side chain and it can be assumed that the Ni(II)-induced hydrolysis of the ligand is already initiated simultaneously with this step.

The Role of Serine in the Nickel(II) Complexes of Hexa- and Hepta-Peptide Containing C-Terminal –SSH-NH_2 Sequence

In the next step, we studied two N-terminally free peptides containing alanine residues at the N-terminal part and -SSH-NH_2 sequence at the C-termini (A_3SSH-NH_2, A_4SSH-NH_2) and investigated them for nickel(II) coordination and preferred binding site, including possible cleavage of the Ala-Ser bond (Figures 1b,c). For these peptides, we could investigate the effect of oligopeptide-like coordination of the N-terminal moiety on the hydrolytic reaction induced by Ni(II) ions, since the formation of a 4 N complex with the -SSH motif is also possible. Both peptides form complexes with the same stoichiometry and similar stability (Table 2) which is not surprising at first glance, since both offer the same coordination environments. In the slightly acidic pH range appears a $[NiL]^{2+}$ species (Figure 4a), which means, that the amino and imidazole groups are deprotonated and coordinated to the metal ion.

This can be deduced from the fact that their stability constants are similar to those of the Ni(II)-GTHS-NH_2 complex, where an (NH_2,N_{im}) binding mode has been described. The low

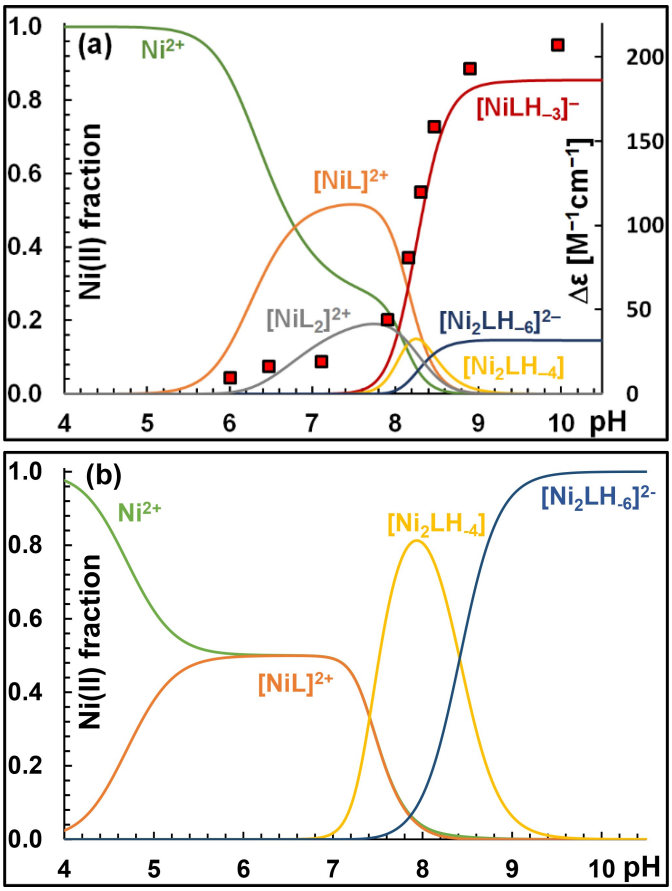

Figure 4. Species distribution curves of the nickel(II) – $A_3SSH\text{-}NH_2$ system at 1:1 (a) and 2:1 (b) metal to ligand ratios and the change in the intensity of molar absorption (λ_{max} = 418 nm) at 1:1 ratio.

absorbance of the sample in the visible range around pH 7 suggests formation of octahedral species, which is consistent with this hypothesis. The monodentate binding of the imidazole nitrogen atom or the terminal amino group results in a lower stability (2.28 for Ac-SKHM-NH_2 and 3.06 for AAAA[22]) than that of the bidentate coordination. The slight difference between the stability of the $[NiL]^{2+}$ species of the $A_3SSH\text{-}NH_2$ and $A_4SSH\text{-}NH_2$ can be explained by the length of the peptide chain, since the farther the two terminal anchors are, the higher the hindrance of macrochelation.[25] $[NiL]^{2+}$ is the dominant complex until pH 8 and the cooperative deprotonation of amide functions occurs in one step, forming $[NiLH_{-3}]^-$, similarly to tetraalanine.

Involvement of amide nitrogens can be concluded from the intense yellow colour of the solution above pH 8 and the maximum of absorbance that can be observed at 418 nm proving the change of complex geometry from octahedral to square planar (Figure 4a).

A single nickel(II) binding can occur at both termini of the ligands; the α-amino and the imidazole nitrogen of histidine can also act as anchoring groups for subsequent backbone nitrogen coordination. (Figure 5a,b). Based on stability data and previous literature results,[25] nickel(II) coordinates predominantly to the N-termini of the peptides, as confirmed by CD spectra shown in Figure S3.[25] Both peptides can bind two metal ions, the heptapeptide is expected to form the $[Ni_2H_{-6}L]^{2-}$ complex, while the hexapeptide is expected to form the $[Ni_2LH_{-5}]^-$ complex as the major species. In the latter case, $A_3SSH\text{-}NH_2$ cannot provide a sufficient number of nitrogen donor atoms to saturate the coordination sphere of the metal ions, so isomeric structures would be proposed for the $[Ni_2LH_{-5}]^-$ complex (Figures 5c,d). Surprisingly, in case of the Ni(II):$A_3SSH\text{-}NH_2$ metal ion excess systems, we observed the formation of $[Ni_2H_{-6}L]^{2-}$ from $[Ni_2H_{-4}L]$ in one step (Figure 4b).

The extra deprotonation process may be due to the loss of H^+ from a coordinated water molecule resulting in a mixed hydroxo complex, but the deprotonation of the C-terminal amide function or even the serine residues cannot be ruled out. Furthermore, deprotonation of the pyrrole nitrogen of the imidazole ring could also be considered, although this would have caused a small change in the UV-Vis and CD spectra (increase in the intensity of the d–d band(s)). The hydrolytic cleavage of the peptide may also be responsible for this phenomenon, although neither the partial nor the complete reaction requires extra hydroxide ions or production of extra proton (Figure S1).

The MS measurement (Figure S4, Table S1) proved that the dinuclear species is coordinated by six times deprotonated form of ligand and it is not a mixed hydroxo complex. The formation of dinuclear species is supported by CD (Figure S5), but the structure of $[Ni_2H_{-6}L]^{2-}$ species cannot be concluded. Figure S5b shows the variation of the CD spectra in basic solution as a function of equivalent of added nickel(II) ion. The series of spectra demonstrates that the shape of CD spectra changes significantly with increasing nickel(II) concentration. However, the CD spectra characteristic for the dinuclear species (1.8 eq. Ni(II)) cannot be obtained from summation of the CD spectra of $(NH_2,(N^-)_{2\ or\ 3})$ and $(N^-)_{3\ or\ 2},N_{im})$ coordinated Ni(II) complexes indicating a different structure for this species. On the other hand, deprotonation processes takes place around pH 8.5 (see Figure 4), which does not suggest that the imidazole nitrogen is replaced by the deprotonated C-terminal amide nitrogen donor atom (this process can usually take place above pH 11).

DFT Calculations

To understand how the unexpected $[Ni_2LH_{-6}]^{2-}$ complex is formed in the Ni(II):$A_3SSH\text{-}NH_2$ = 2:1 system by an additional deprotonation process instead of $[Ni_2LH_{-5}]^-$, quantum chemical calculations were performed. Our aim was to determine the thermodynamically most stable isomer, which should be most likely to form at the high pH range in aqueous solution, as proton transfer reactions occur via very low barriers, and thus thermodynamic control should prevail in the process.

Three isomers of $[Ni_2LH_{-6}]^{2-}$ were generated as starting structures for the subsequent calculations (Figure S6). The five deprotonation sites (amide nitrogens) were identical in all isomers, while the sixth was chosen to be the pyrrolic hydrogen atom of the histidine (isomer B), the hydroxyl hydrogen atom of

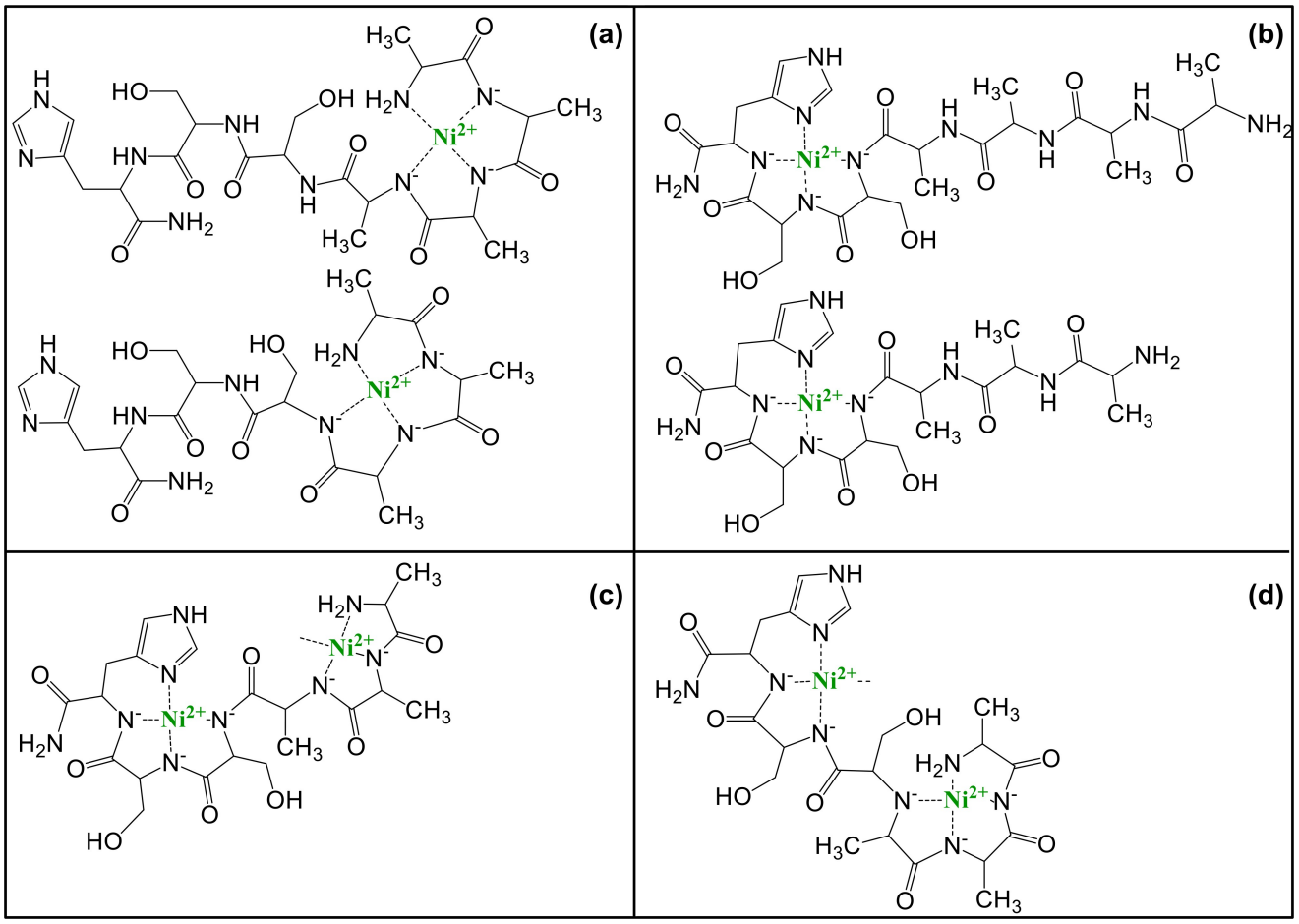

Figure 5. Amino terminal (a) and -SSH-NH_2 coordinated $[NiH_{-3}L]^-$ complex (b) of the ligands A_4SSH-NH_2 and A_3SSH-NH_2 and the unsaturated coordination sphere of nickel(II) in the possible coordination isomers of the hypothetic $[Ni_2H_{-5}L]^-$ species of A_3SSH-NH_2 (c and d).

the fourth (isomer A) or fifth serine (isomer C) of the peptide. After a systematic conformational search, the most stable conformer for each isomer was found. In these structures, the nickel atoms exhibited their characteristic square planar orientation of the ligands.

Interestingly, according to the relative energies obtained by DFT, the most stable structure was found to be isomer A1, followed by A2 and B (Figure 6). The significant energy differences suggest that in solution isomer A1 is dominant, showing a clear preference for the deprotonation of the hydroxyl group in the side chain at the fourth serine amino acid of the hexapeptide.

The bond orders in the environment of nickel atoms can be seen in the table (Table S2) below. The range of the obtained data is between 0.5207–0.7193, where the Ni–N bonds were 0.61(±9), and surprisingly the Ni–O bond were even stronger with the 0.71 value, according to our calculations.

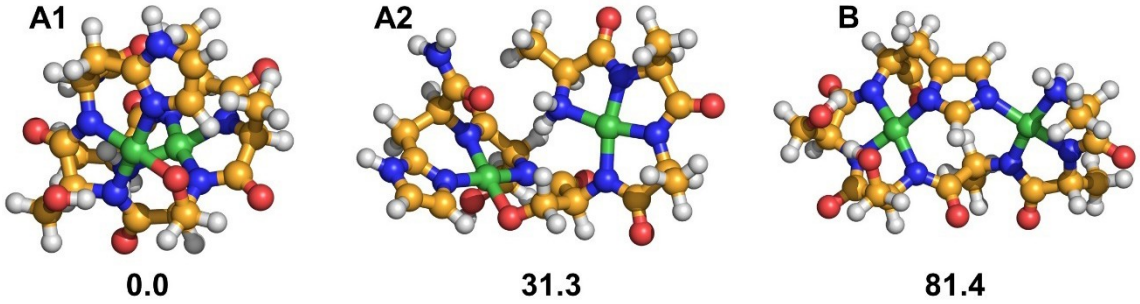

Figure 6. The most stable optimized conformers of the $[Ni_2LH_{-6}]^{2-}$ complexes (C: orange, N: blue, O: red, Ni: green, H: while), and their relative energies in [kJ mol^{-1}] units.

The other part of Table S2 summarizes the angles in the environment of Ni atoms. In a square planar Ni(II) complex the angles should be ≈90°, and the sum of them close to 360°, which criterium is met in all cases, but it is important to note that the most accurate angles was observed in case of A1 structure, with the one which provides the best geometry and the best match with the measured CD spectrum.

According to the results from the TD-DFT calculations we can say with confidence that the most stable $[Ni_2LH_{-6}]^{2-}$ isomer is the A1, where the fourth serine hydroxyl group undergoes deprotonation.

Ni(II) Induced Hydrolytic Processes of $A_4SSH\text{-}NH_2$

Analysis of CD spectra of nickel(II) and $A_4SSH\text{-}NH_2$ containing systems (Figure 7) can help to identify the preferred binding site of the peptide. In neutral and slightly basic medium, no or minimal CD activity can be observed, strengthening the formation of a macrochelate structure instead of an amide-coordinated one. The heptapeptide offers a (NH_2,3 N^-) and a (3 N^-,N_{im}) binding site at high pH.

The registered CD curve of the equimolar solution of nickel(II) and $A_4SSH\text{-}NH_2$ cannot be obtained from the CD spectra of $[NiH_{-3}L]$ complexes coordinated to (NH_2,3 N^-) (AAAA) and (3 N^-,N_{im}) (Ac-MKHM-NH_2) donor set. However, a similar curve to the CD spectrum of the $[NiH_{-3}L]^-$ complex of $A_4SSH\text{-}NH_2$ is obtained by summing those of AAAA and Ac-KGGYTMHK-NH_2 peptides in a 70:30 ratio. Similarly, the CD spectrum of the $[Ni_2H_{-6}L]^{2-}$ complex can be approximated by summing the CD spectra of the above two peptides in 50:50 ratio. The peptide used as a model contains a -TKHM- sequence, whose $[NiH_{-3}L]$ complex has a different CD spectrum from that of peptides not containing threonine.[15,25] These data suggest that the N-terminal region is the more occupied in equimolar solution, while in the presence of a double excess of metal ions, nickel(II) ions bind equally to both binding sites of the molecule.

Since both in the equimolar system and in the solution containing the metal ion in excess, a complex in which the metal ion binds to the –SXH- sequence via (3 N^-,N_{im}) coordination is present in the alkaline range, hydrolytic processes are expected to occur. HPLC measurements were carried out to get insights on the non-reversible reactions, namely, the selective hydrolytic process. The chromatograms (Figure 8) clearly show the appearance of new peaks at 4.9 and 9.6 min besides that of the initial ligand at 10.0 min, after the addition of excess of nickel(II) ions and base to set the pH to around 8.

The new compounds corresponding to these peaks should be more polar and/or smaller than the heptapeptide, as it is suggested for the nickel(II)-assisted cleavage. Identification of the two products was carried out with HPLC standards and with the help of mass spectra of a sample at pH 8 having 2:1 metal to ligand ratio (Figure 9, Table S3). Besides the species $[Ni_2H_{-6}L]^{2-}$, a compound with the identical composition of the $[NiH_{-3}L]^-$ complex of the AAAA fragment could also be observed, supporting the specific cleavage of the peptide between the serine and alanine residues, forming a tetraalanine molecule with free terminal carboxylate group.

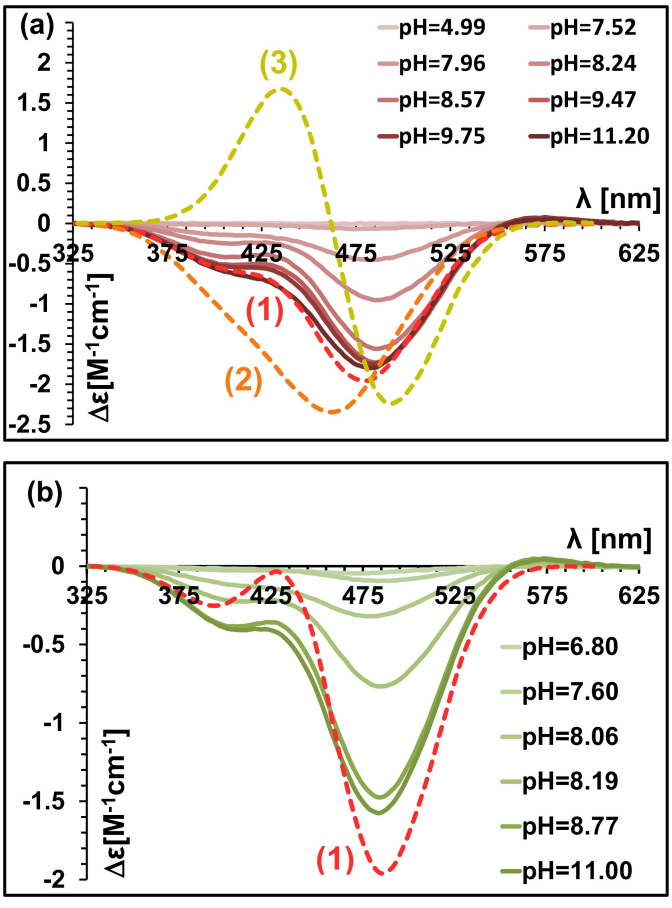

Figure 7. Series of CD spectra depending on pH of the equimolar system, CD spectra of $NiH_{-3}L$ species of AAAA (2), Ac-KGGYTMHK-NH_2[27] (3) and the model curve of $[NiH_{-3}L]^-$ of $A_4SSH\text{-}NH_2$ peptide, calculated by summing the CD curves of AAAA and Ac-KGGYTMHK-NH_2 (1) at a ratio of 70%:30% (a); series of CD spectra depending on pH at double nickel(II) ion excess and the model curve of the $[Ni_2H_{-6}L]$ of A4SSH-NH_2 peptide (1) calculated by summing the CD curves of AAAA and Ac-KGGYTMHK-NH_2 at a ratio of 50%:50% (b).

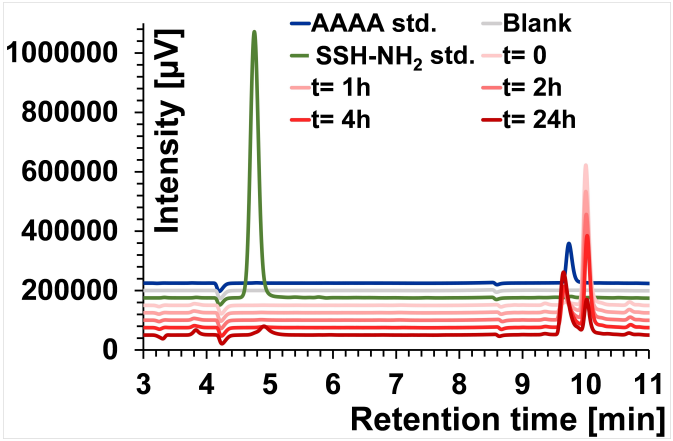

Figure 8. Series of time dependence HPLC chromatograms of the Ni(II): AAAASSH-NH_2 2:1 ratio system at pH = 8.23.

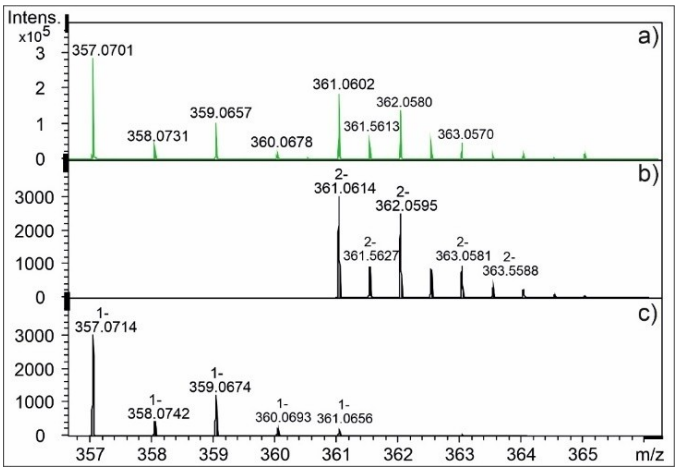

Figure 9. Mass spectra of the nickel(II) – $A_4SSH\text{-}NH_2$ system at 2:1 ratio, pH = 8.24 (a) and the simulated spectra of the dinuclear $[Ni_2H_{-6}L]^{2-}$ species (b) and the formed hydrolysis product (c), the $[NiH_{-3}L]^{2-}$ complex of AAAA (H^+ adduct).

The mass spectra and the HPLC proves the presence of the hydrolysis of the AAAASSH-NH_2 peptide, in case of the 2:1 and the 1:1 ratio system, which spontaneously occurs under the conditions of the solution equilibrium; T = 25 °C, pH = 8.23 and a few hours enough to detect the products of the specific cleavage process.

Metal Binding Concepts of the Intermediate Ester Formed in the Hydrolytic Process–A Model Ligand, AAAεKSH-NH_2

As it was stated above, one of the internal steps of the specific cleavage mechanism is the formation of an ester/amine derivative of the original ligand (Scheme 1 and Figure S1). It means for the investigated ligand AAAASSH-NH_2 that this intermediate contains the two metal binding sites of the hydrolysis products in a single molecule at this point of the process. Unfortunately, the complex formation behaviour of this ester derivative cannot be described easily due to the ongoing hydrolysis of the ester bond even during the examinations. To overcome this obstacle, we synthesized ligand AAAεKSH-NH_2, by building in a side chain coupled lysine residue in the sequence, and thereby eliminating the ester bond while maintaining the same donor atoms. Moreover, the number of atoms between the two metal binding sites of the ligand is the same, but the ester bond is replaced by a butylene group (see Figure S8).

Deprotonation processes of the ligand can be described as shown in Table 1, where the lowest p*K* corresponds to the histidine imidazole group and the higher values belong to the two amino groups. The 6.27 p*K* value for histidine is in good agreement with other peptides containing one histidine. However, the deprotonation constants of the two ammonium groups cannot be assigned by comparison with the corresponding values in other peptides.

^{1}H NMR spectra were also measured to ensure the assignment of p*K* values to functional groups. (Figure S9). It was confirmed by the change of the chemical shift of histidine side chain (–CH) protons at pD 6.62 by adding base that the lowest p*K* corresponds to the dissociation of the imidazolium function. It was also concluded that by pD 8.36, NMR signals of the ($-CH_3$) hydrogens of N-terminal alanine begin to shift toward lower values, proving that the lower p*K* value is related to the N-terminal (Ala1) ammonium group while the deprotonation of lysine ($-NH_3^+$) occurs at higher pH value.

Using pH potentiometry, we aimed to describe the nickel complex formation processes of the ligand, however, the measurements took quite a long time, which is not surprising, since complex formation equilibria are slow to establish in case of Ni(II)-oligopeptide systems. For this reason, the error of the determined stability constants is larger, then those of other studied peptides. However, it can be unambiguously seen on the species distribution curves, that the nickel(II) complexes are present above pH 5, similarly to other albumin-like ligands. (Figure 10)

According to the stability constants, no $[NiL]^{2+}$ or $[NiHL]^{3+}$ species with (NH_2,N_{im}) coordination mode can be calculated, in contrast to the GTHS-NH_2 (or MKHM-NH_2) model peptides. Formation of $[NiH_{-1}L]^+$, however can be deduced from titration data, meaning an extra loss of H^+ ion from the ligand. At first

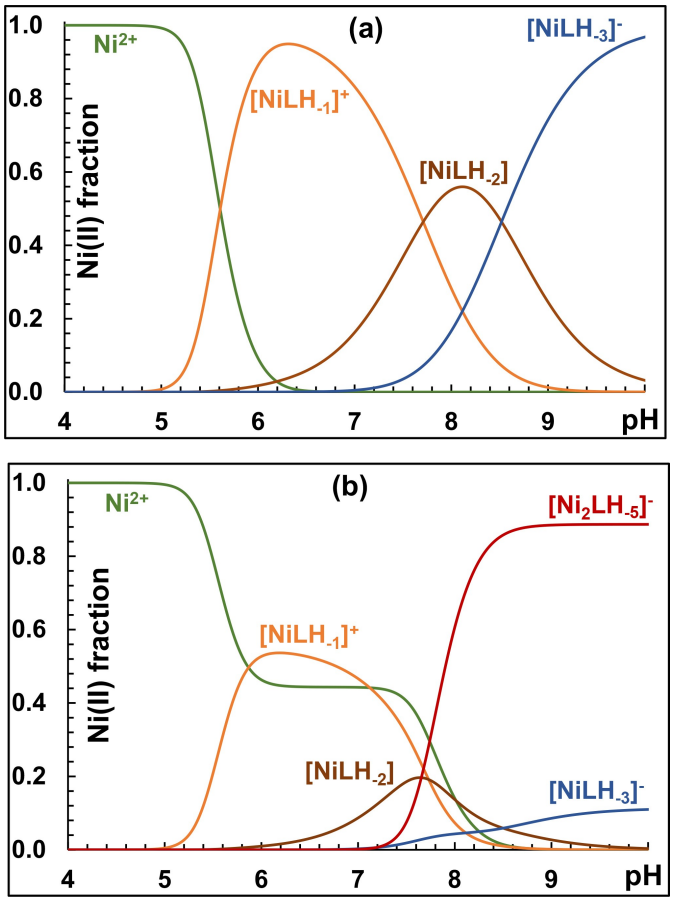

Figure 10. Distribution curves of the systems Ni(II):AAAεKSH-NH_2 = 1:1 (a) and 2:1 (b).

sight, it would mean the deprotonation of one amide function and all three functions occur. However, a species with the stoichiometry of $[NiH_{-2}LH]^+$ is more plausible, since the formation of an albumin-like (NH_2,2 N^-,N_{im}) binding is highly preferred, while the N-terminal ammonium function of Ala1 is protonated. The low pH range in which the complex is formed also supports this hypothesis, since nickel(II) complexes formed by the binding of the N-terminal amino anchor and subsequent amide donors exist only around pH 8. However, the derived equilibrium constant for the $[NiH_{-2}LH]^+$ complex of AAAεKSH-NH_2 ($\log K = \log\beta(NiH_{-2}LH) - \log\beta(HL) = 2.35 - 8.11 = -5.76$) is increased compared to that of the model GTHS-NH_2 having a stability constant of −6.45 for the albumin-like coordinated nickel(II) ion.

Further deprotonation of the ligand results in the appearance of $[NiH_{-2}L]$ which can have two coordination isomers: (i) either the uncoordinated amino group is deprotonated or (ii) by rearrangement of the coordination sphere of the nickel(II) ion, the nickel(II) is bound to the N-terminal amino group, the two subsequent amide nitrogen atoms and the imidazole group of histidine. The corresponding pK value (7.56) is close to $pK_{(NH2)} = 7.40$ value of the free ligand suggesting the majority of albumin-like coordinated species. Above pH 10, a new extra base consuming process occurs resulting in the formation of $[NiH_{-3}L]^-$ complex. A similar deprotonation process was observed for the Ni(II)-GTHS-NH_2 system, and this deprotonation step is attributed to the deprotonation of pyrrole type NH group of imidazole ring (pK = 11.15, see Table 2).[23] In our case, this deprotonation step can be characterized with a lower pK value (pK = 10.26), which could be an averaged value of the pK_{amid3} for (NH_2,3 N^-) coordinated isomer and the pK_3 value of pyrrole type NH group in the albumin-like coordinated isomer (see later, at the analysis of CD spectra). Calculated distribution curves of Ni(II)-AAAA-GTHS-NH_2 = 1 : 1 : 1 system modelling the two metal binding sites of the ligand also confirms the strong preference for the albumin-like binding site of the molecule.

Similar species formation can be observed at 1 : 2 metal to ligand ratio. As shown in Figure 10, the deprotonation of only five amide groups occurs after the formation of an albumin- and a tetraalanine-like binding resulting in the saturation of the coordination spheres of both nickel(II) ions ($[Ni_2H_{-5}L]^-$).

As it can be deduced from the evaluation of pH potentiometric data, structural isomers are likely to form in case of equimolar solution. To establish which metal binding site plays a major role in coordination, circular dichroism spectra were recorded. The lowest pH, at which CD active Ni(II) species are formed is 5.5, in agreement with the formation of the albumin-like coordinated complexes also from the aspect of the shape of the CD curve (Figure S11a).

These observations suggest the coordination of the –KSH– sequence above pH 5. The position of the CD bands does not change by increasing pH, but the significant increasing of the CD extrema between pH 6–9 supports the existence of two coordination isomers. A comparison of the CD spectra of the two types of the nickel(II) complex (albumin- and oligopeptide-like coordinated) suggests that by pH 9 the ratio of (NH_2,2 N^-,N_{im}) to (NH_2,3 N^-) coordinated complexes is 80 %:20 %. However, further increase in pH does not result in any change in the spectra, confirming that the ratio of albumin-like to oligopeptide-like coordinated isomers does not change further. This agrees with the assumption that in the (NH_2,2 N^-,N_{im}) coordinated complex, the deprotonation of the pyrrole-type NH group of the coordinated imidazole ring occurs in the last deprotonation step.

^{1}H NMR studies reveal that at 1 to 1 ratio of metal and ligand at pD = 6.55, aromatic CH protons of the imidazole ring of histidine shifts toward lower chemical shift values from 8.48 ppm to 7.42 ppm and no other NMR peaks appear in this range. A significant change can be seen in the -CH protons in case of His and Ser also due to the formed complex in the C-terminal region. These observations lead to the conclusion that all the nickel ions bind to the C-terminal part of the ligand and N-terminally coordinated metal ions are absent at this pD value. In basic medium, at pD = 10.82, similar consequences can be drawn; the nickel binding occurs at the C-terminal part of the peptide, just the small amount of the -CH_3 multiplets, belonging to the N-terminally alanine (Ala1)- moved to lower chemical shift as the pD increased (Figure S12).

At twofold metal ion excess, both metal binding sites are expected to be involved in the complex formation. The binding of nickel(II) ions to both binding sites of the molecule is clearly demonstrated by CD spectra. (Figure S11b). Until pH 7 the CD spectra are similar to those of equimolar solution, corresponding to the formation of mononuclear species with (NH_2,2 N^-,N_{im}) coordination mode. Addition of more base to the sample results in the drop of the positive CD band at 400 nm indicating the presence of another coordination mode above pH 8, simultaneously with the formation of the $[Ni_2H_{-5}L]^-$.

Figure 11 shows the CD spectra of the mononuclear (Figure 11a) and dinuclear Ni(II) complexes (Figure 11b) present in the pH 8.7–9.3 range for the AAASSH-NH_2, AAAASSH-NH_2, and AAAεKSH-NH_2 peptides together. A comparison of the spectra shows that the spectra of the model peptide registered in 1 : 1 and 2 : 1 Ni(II)-ligand ratios differ from those of both hexa- and heptapeptide. These differences also support that during the equilibrium measurements hydrolysis does not take place or negligible and the presence of the intermediate ester is not detectable in the case of hexa- and hepta-peptides containing –SSH– sequence.

Experimental Details

Peptide Synthesis and Other Materials

The Ac-SKHM-NH_2 peptide was previously synthesized as described in a previous article.[22] The synthesis of other three peptides (A_4SSH-NH_2, A_3SSH-NH_2, AAAεKSH-NH_2) were performed with solid phase peptide synthesis by using a microwave-assisted Liberty 1 Peptide Synthesizer with an UV-monitoring system (CEM, Matthews, NC). The TBTU/HOBt/DIPEA activation strategy was applied to connect the amino acid derivates on the Rink Amide AM resin, using the Fmoc/*t*Bu technique. It is important to note that in the synthesis of the AAAεKSH-NH_2 peptide we used the inverted version (εLys, Boc-Lys(Fmoc)–OH) of the classic lysine (Lys, (Fmoc-Lys(Boc)-OH) amino acid. With the application of this εLys, its side

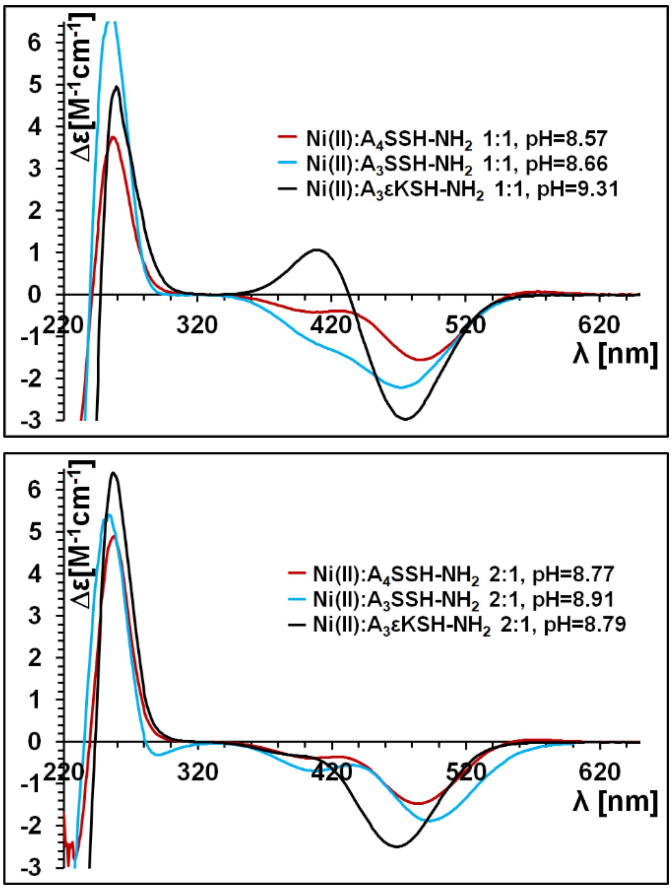

Figure 11. Comparison of the CD spectra of metal complexes formed at alkaline pH in the Ni(II)-ligand 1:1 (a) and 2:1 ratio (b).

chain can be activated, and we were able to couple the three alanine amino acids there. 30 Watts microwave power was used for 180 s at 75 °C to remove the Fmoc protecting group by means of 20 V/V% piperidine and 0.1 M HOBt·H_2O in DMF.

Coupling of the amino acids was carried out using excess of amino acids at 75 °C with 30 Watts microwave power for 300 s while reacting with 0.5 M HOBt and 0.5 M TBTU in DMF and 2 M DIPEA in NMP as activating reagents. At the end of the synthesis the Fmoc group of the N-terminus of the peptide sequence was also removed. Using a mixture of TFA/TIS/H_2O/2,2′-(ethylenedioxy)diethanethiol (94/2.5/2.5/1 V/V) for 2 h at room temperature the peptides were cleaved from the resins and simultaneously the side chain protective groups were also removed. Each peptide solved in trifluoroacetic acid was filtered from the resin and precipitated by cold diethyl ether to recover. The solid product was also washed with cold diethyl ether and after separation dried, dissolved in water, and finally frozen for lyophilization.

Analytical RP-HPLC analyses were performed using a Jasco instrument equipped with a Jasco MD-2010 plus multiwavelength detector monitoring the absorbance at 222 nm to check the purity of the synthesized peptides. Gradient elution 0–25-0 of solvent A was carried out using solvent A (0.1 V/V% TFA in water) and solvent B (0.1 V/V% TFA in acetonitrile) at a flow rate of 0.8 ml/min applying a Teknokroma EUROPA PROTEIN C18 chromatographic column (250×4.6 mm, 300 Å pore size, 5 μm particle size) and Teknokroma EUROPA PROTEIN C8 chromatographic column (250×4.6 mm, 300 Å pore size, 5 μm particle size). The active substance content of the peptides was greater than 91% for each product, confirmed by pH-potentiometric measurements, too, identifying the protonation sites. The ESI-MS measurements registered in positive mode and showed the exact molecular weight of the synthetized ligands.

All solvents and chemicals used for synthesis were obtained from commercial sources in the highest available purity and used without further purification. The N-fluorenylmethoxycarbonyl (Fmoc)-protected amino acids (Fmoc-Ala-OH, Fmoc-Ser(tBu)-OH, Fmoc-His(Trt)-OH, Fmoc-Lys(Boc)-OH and Boc-Lys(Fmoc)-OH), 2-(1-H-benzotriazole-1-yl)-1,1,3,3-tetramethyluronium tetrafluoroborate (TBTU) and the Rink Amide AM resin were purchased from Novabiochem (Switzerland). N,N-diisopropyl-ethylamine (DIEA) and trifluoroacetic acid (TFA) were Merck products, while N-hydroxybenzotriazole (HOBt), N-methyl-pyrrolidone (NMP), triisopropylsilane (TIS), 2,2′-(ethylenedioxy)diethanethiol (DODT) and 2-methyl-2-butanol were from Sigma-Aldrich. Piperidine, acetic acid (AcOH), diethyl ether (Et_2O) and dichloromethane (DCM) were Molar solvents as well as acetonitrile (ACN) and peptide-synthesis grade N,N-dimethylformamide (DMF) and acetic anhydride were purchased from VWR.

Analytical grade reagent of $NiCl_2$ were used to prepare the metal ion stock solution and gravimetry was proved the concentration via the precipitation of oxinates.

Potentiometric Measurements

MOLSPIN pH-meter was applied to carry out the titrations equipped with a 6.0234.100 combination glass electrode (Metrohm) and a MOL-ACS microburette controlled by a computer. The pH-potentiometric measurements were carried out at 298 K and at a constant ionic strength of 0.2 M KCl using carbonate-free stock solution of potassium-hydroxide with a known exact concentration of around 0.2 M. Argon gas was applied above the solutions during the titrations to avoid the presence of carbon dioxide and dioxygen and a VELP Scientific magnetic stirrer was used to homogenize the samples. Ligand concentration was set in the range of 1.5×10^{-3}–2.0×10^{-3} M in the titrated samples with the initial volume of 4 cm^3 and the examined metal to ligand ratios were 1:2, 1:1 and 2:1. Investigations about the reversibility of the systems was also proven by this technique using the following method: after the end of titration the system has been moved to the initial (acidic) pH in minutes and then the titration was repeated without taking apart the titration system.

Corrections have been made to eliminate the diffusion potential by determining and subtracting the Irving factor from the measured pH values.[28] The recorded pH readings were converted to hydrogen ion concentration. Protonation constants of the ligands and overall stability constants (log β_{pqrs}) of the metal complexes were calculated by means of the general computational programs (PSEQUAD and SUPERQUAD) as described in our previous publications.[29,30] Equations (1) and (2) define the equilibrium constants for the binary systems.

$$pM + qH + rL \rightleftharpoons M_pH_qL_r \quad (1)$$

$$\beta_{pqr} = \frac{[M_pH_qL_r]}{[M]^p \cdot [H]^q \cdot [L]^r} \quad (2)$$

Spectroscopic Measurements

The same concentration range as used for pH-potentiometry was selected to register the UV-Vis spectra of the nickel(II) complexes. A

VWR UV-1600PC spectrophotometer was applied in the wavelength range of 250–1100 nm for nickel(II) complexes.

A JASCO J-810 spectropolarimeter was used to record the CD spectra of the same complexes from 280 to 800 nm using 1 and/or 10 mm cells and the same concentrations as used for pH-potentiometric measurements.

A Bruker maXis II QTOF ESI-TOF instrument was applied to carry out the ESI-TOF-MS analyses in positive mode and the ligands were solved in water at the concentration of 1×10^{-4} M.

A Bruker AVANCE I 400 MHz NMR instrument was used to determine the order in the pK values belonging to the AAAεKSH-NH_2 ligand, moreover because of usually the nickel(II) forms square planar- and diamagnetic complexes after the N_{amide} deprotonation of peptide backbone, therefore we could also apply this technique to determine the environments of some of the forming complexes according to the change in the chemical shift at different pD values. In each cases the solvent was D_2O, the pD values were settled with NaOD and DCl and the concentration of the ligand was 4 mM.

Reverse-Phase High Performance Liquid Chromatography Measurements

The application of the RP-HPLC technique was not just important to prove the purity of the synthesized peptides but also to prove the presence of the assumed metal ion induced hydrolytic process. For this investigation the same, Jasco instrument was used monitoring the wavelength on 222 nm with the Jasco MD-2010 plus multiwavelength detector. Gradient elution with 0–25–0 % of solvent A and isocratic elution 3 % of solvent A were carried out using solvent A (0.1 V/V% TFA in water) and solvent B (0.1 V/V% TFA in acetonitrile) at a flow rate of 0.8 ml/min applying a Teknokroma EUROPA PROTEIN C18 chromatographic column (250×4.6 mm, 300 Å pore size, 5 μm particle size) and Teknokroma EUROPA PROTEIN C8 chromatographic column (250×4.6 mm, 300 Å pore size, 5 μm particle size).

Computational Methods

Each investigated structure underwent an initial geometry optimization with the semi-empirical GFN2-xTB method, using default settings and a GBSA solvation model for water. On the obtained minima, a conformational search was performed with the Crest[31] program with a default setup using the same solvation model, locating the lowest energy geometries on the potential energy surface. The structures were fully optimized at the B3LYP–D4/def2-SVP level of theory with the CPCM solvation model for water, employing the Orca program package[32] version 5.0.0. All eigenvalues of the Hessian were positive values for each structure, confirming that the located critical points are minima of the potential energy surface. TD-DFT calculations were performed on the minima, using the ωB97X–D4/def2-TZVP method with the CPCM water model with NROOTS 25 and TDA false settings.

Conclusions

The side chain of histidine serves as the metal ion binding site for many native proteins, and very often histidine is present in a specific amino acid environment. Such a specific environment is the –(S/T)XH– sequence, in which case the peptide bond preceding serine or threonine has been previously shown to hydrolyse in the presence of twofold nickel(II) excess at 45–50 °C in an alkaline medium (above pH 8) in many cases after several hours.

In present study, we therefore sought to determine whether Ni(II)-induced hydrolysis also occurs under conditions of potentiometric measurements (25 °C) and during their duration, which may affect the values of the stability constants determined from equilibrium measurements.

These investigations were carried out with the peptides Ac-SKHM-NH_2, A_3SSH-NH_2, and A_4SSH-NH_2. Moreover, we synthesized the peptide AAAεKSH-NH_2, which was the model of the intermediate ester according to the mechanism of the hydrolysis.

The following conclusions were drawn from the results:

(i) The peptide Ac-SKHM-NH_2 hydrolyses in alkaline medium in the presence of Ni(II) already at 25 °C in a short time, yielding SKHM-NH_2 peptide and acetate ion, consistent with the previously described mechanism. This process, however, is negligible at 25 °C in equimolar solution, pH ≈8.5, so the composition and stability constants of the complexes formed in this range are reliable.

(ii) In the case of the peptides A_3SSH-NH_2 and A_4SSH-NH_2 in equimolar solution, majority of Ni(II) is coordinated by the N-terminal part of the peptide in a tetraalanine-like coordination mode. As a result, Ni(II)-induced hydrolysis could not be observed under the conditions of the potentiometric study, because the $[NiH_{-3}L]^-$ complex in the environment of the –SXH– motif is required for hydrolysis.

(iii) The hydrolysis of the A_3SSH-NH_2 peptide was not observed in the presence of excess metal ions. This can be explained by the absence of a 4 N-coordinated nickel(II) complex of the -SSH- sequence in the dinuclear complex. Theoretical, DFT calculations on the structure of $[Ni_2H_{-6}L]^{2-}$ complex–detected by potentiometric and MS measurements–confirmed that the fourth coordination site of the Ni(II) ion bound to the C-terminal part is occupied by the deprotonated seryl-O^-.

(iv) In the case of A_4SSH-NH_2, both Ni(II) ions in the dinuclear complexes bind with 4 N coordination mode, thus fulfilling the conditions for hydrolysis. HPLC analyses at pH ≈8.2 confirmed the presence of the hydrolysis products at 25 °C, thus the composition and stability constants of the complexes formed in the alkaline range can only be estimated. As the Ni(II) preferred binding site is the N-terminus of the ligand, the composition and stability constants of the mononuclear complexes formed in equimolar system can be reliably determined until the slightly basic pH.

(v) Based on the investigation of the Ni(II) complexes of the model peptide AAAεKSH-NH_2, it was concluded that in the physiological pH range (pH 6–8), the metal ion binds to the –εKSH-sequence of the molecule with albumin-like coordination mode. Dinuclear complexes are formed at a 2:1 Ni(II)-ligand ratio, where the coordination mode of the two

metal ions is tetraalanine- or albumin-like. Thus, the spectral data obtained for the Ni(II) complexes of this model peptide correspond to the expected spectral data for the Ni(II) species of intermediate ester. The differences between the CD spectra of this model peptide and those of hexa- and hepta-peptides also support that during the equilibrium measurements hydrolysis is does not take place or negligible and the presence of the intermediate ester is not detectable in the case of hexa- and hepta-peptides containing –SSH– sequence in equimolar solution.

These results help to understand the unusual spectral parameters obtained in previous studies of nickel(II) complexes of prion and tau protein fragments and to better clarify the role of serine or threonine in the vicinity of histidine. On the other hand, it has been shown that nickel(II) induced hydrolysis can take place at room temperatures and even in equimolar solutions. The hydrolysis can be monitored by CD spectroscopy and HPLC technique, and the measurement conditions that could be used for the further analysis of native protein fragments containing the –(S/T)XH– sequence have been defined.

Supporting Information

The authors have not cited additional references within the Supporting Information

Acknowledgements

This research was supported by the University of Debrecen Program for Scientific Publication. The financial support for O.H. by the National Research, Development and Innovation Office through the project OTKA-FK 138823 is gratefully acknowledged. Furthermore, O.H. is grateful for the support from the János Bolyai Research Scholarship of the Hungarian Academy of Sciences, and the ÚNKP-22-5 and ÚNKP-23-5 New National Excellence Program from the National Research, Development and Innovation Fund. The authors thank the Vienna Supercomputing Center and the Governmental Information Technology Development Agency (KIFÜ) for the CPU time that has been used for this project.

Conflict of Interests

The authors declare no conflict of interest.

Data Availability Statement

The data that support the findings of this study are available from the corresponding author upon reasonable request.

Keywords: DFT calculations · Ni(II) complexes · Ni(II) induced hydrolysis · Peptides · Stability constants

[1] I. E. Burgeson, N. M. Kostić, *Inorg. Chem.* **1991**, *30*, 4299.
[2] X. Chen, L. Zhu, H. Yan, X. You, N. M. Kostić, *J. Chem. Soc. Dalton Trans.* **1996**, 2653.
[3] N. M. Milović, N. M. Kostić, *Metal Ions in Biological Systems*, (Eds. A. Sigel, H. Sigel), Marcel Dekker Inc., **2001**, Vol. *38*, pp. 145–186.
[4] N. M. Milović, N. M. Kostić, *J. Am. Chem. Soc.* **2003**, *125*, 781.
[5] S. Rajković, M. D. Živković, M. I. Djuran, *Curr. Protein Pept. Sci.* **2016**, *17*, 95.
[6] G. Allen, R. O. Campbell, *Int. J. Pept. Protein Res.* **1996**, *48*, 265.
[7] A. Belczyk-Ciesielska, I. Zawisza, M. Mita, A. Bonna, W. Bal, *Inorg. Chem.* **2014**, *53*, 4639.
[8] M. Yashiro, Y. Sonobe, A. Yamamura, T. Takarada, M. Komiyama, *Org. Biomol. Chem.* **2003**, *1*, 629.
[9] W. Bal, J. Lukszo, K. Bialkowski, K. S. Kasprzak, *Chem. Res. Toxicol.* **1998**, *11*, 1014.
[10] E. Kopera, A. Krężel, A. M. Protas, A. Belczyk, A. Bonna, A. Wysłouch-Cieszyńska, J. Poznański, W. Bal, *Inorg. Chem.* **2010**, *49* (14), 6636.
[11] A. Krężel, E. Kopera, A. M. Protas, J. Poznański, A. Wysłouch-Cieszyńska, *J. Am. Chem. Soc.* **2010**, *132* (10), 3355.
[12] E. I. Podobas, A. Bonna, A. Polkowska-Nowakowska, W. Bal, *J. Inorg. Biochem.* **2014**, *136*, 107.
[13] A. M. Protas, H. H. Ariani, A. Bonna, A. Polkowska-Nowakowska, J. Poznański, W. Bal, *J. Inorg. Biochem.* **2013**, *127*, 99.
[14] E. I. Podobas, D. Gutowska-Owsiak, S. Moretti, J. Poznanski, M. Kulinczak, M. Grynberg, A. Gruca, A. Bonna, D. Plonka, T. Fraczyk, G. Ogg, W. Bal, *Front. Mol. Biol. Sci.* **2022**, *9*, 828674.
[15] M. Mylonas, A. Krezel, J. C. Plakatouras, N. Hadjiliadis, W. Bal, *J. Chem. Soc. Dalton Trans.* **2002**, *22*, 4296.
[16] M. Mylonas, J. C. Plakatouras, N. Hadjiliadis, *Dalton Trans.* **2004**, 4152.
[17] N. E. Wezynfeld, T. Frączyk, A. Bonna, W. Bal, *Metallomics* **2020**, *12*, 649.
[18] E. Kopera, A. Belczyk-Ciesielska, W. Bal, *PLoS One* **2012**, *7*, e36350.
[19] E. Kurowska, J. Sasin-Kurowska, A. Bonna, M. Grynberg, J. Poznański, L. Knizewski, K. Ginalski, W. Bal, *Metallomics* **2011**, *3*, 1227.
[20] N. E. Wezynfeld, K. Bossak, W. Goch, A. Bonna, W. Bal, T. Frączyk, *Chem. Res. Toxicol.* **2014**, *27* (11), 1996.
[21] A. Belczyk-Ciesielska, B. Csipak, B. Hajdu, A. Sparavier, M. N. Asaka, K. Nagata, B. Gyurcsik, W. Bal, *Metallomics* **2018**, *10*, 1089.
[22] C. Kállay, I. Turi, S. Timári, Z. Nagy, D. Sanna, G. Pappalardo, P. de Bona, E. Rizzarelli, I. Sóvágó, *Monatsh. Chem.* **2011**, *142*, 411.
[23] I. Turi, D. Sanna, E. Garribba, G. Pappalardo, I. Sóvágó, *Polyhedron* **2013**, *62*, 7.
[24] W. Bal, H. Kozlowski, R. Robbins, L. D. Pettit, *Inorg. Chim. Acta* **1995**, *231*, 7.
[25] I. Sóvágó, K. Várnagy, K. Ősz, *Comments Inorg. Chem.* **2002**, *23* (2), 149.
[26] T. Frączyk, A. Bonna, E. Stefaniak, N. E. Wezynfeld, W. Bal, *Chem. Biodiversity* **2020**, *17*, e1900652.
[27] B. D. Balogh, G. Szunyog, M. Lukács, B. Szakács, I. Sóvágó, K. Várnagy, *Dalton Trans.* **2021**, *50*, 14411.
[28] H. M. Irving, M. C. Miles, L. D. Pettit, *Anal. Chim. Acta* **1967**, *38*, 475.
[29] L. Zékány, I. Nagypál, D. Legett, *Plenum Press*, New York, **1985**, p. 291
[30] P. Gans, A. Sabatini, A. Vacca, *J. Chem. Soc. Dalton Trans.* **1985**, *6*, 1195.
[31] P. Pracht, F. Bohle, S. Grimme, *Phys. Chem. Chem. Phys.* **2020**, *22*, 7169.
[32] F. Neese, *Wiley Interdiscip. Rev.: Comput. Mol. Sci.* **2012**, *2*, 73.

Manuscript received: May 30, 2024
Revised manuscript received: July 10, 2024
Accepted manuscript online: July 12, 2024
Version of record online: ■■, ■■

RESEARCH ARTICLE

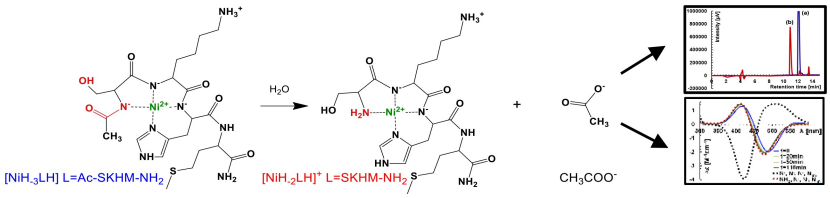

We have shown that nickel(II)-induced hydrolysis of peptides containing –(S/T)XH– can take place at room temperatures in equimolar solutions. The hydrolysis can be monitored by CD spectroscopy and HPLC technique, and the measurement conditions that can be used for the further analysis of native protein fragments containing the –(S/T)XH– sequence have been determined.

*B. Sándor, Á. Grenács, L. Nagy, O. Hollóczki, K. Várnagy**